

# Scaling Laws for the Magnetic Components in Galvanically Isolated Single-Stage Multi-Level Converter Systems

Dr. Jannik Schäfer  
Power Electronic Systems Laboratory  
ETH Zurich  
Zurich, Switzerland  
schaefer@lem.ee.ethz.ch

Prof. Dr. Johann W. Kolar  
Power Electronic Systems Laboratory  
ETH Zurich  
Zurich, Switzerland  
kolar@lem.ee.ethz.ch

In order to reduce the volume of the filter components at the input or at the output of non-isolated DC/DC converter stages, so-called multi-level (ML) converter topologies are used more and more often, which, by connecting several identical converter cells in series, reduce e.g. the voltage-time areas across inductors, whereby they have to store less energy and can therefore also be built smaller in volume. The advantages of this ML approach have often been proven by means of realized hardware demonstrators with remarkable power densities, but only for systems without galvanic isolation. In order to show why the ML approach is so rarely seen in galvanically isolated systems, and why it is not reasonable to be used in such systems even from a conceptional point of view, scaling laws for the magnetic components in galvanically isolated ML converter systems are derived in this paper, which are then used to investigate how the volumes of the different magnetic components change with increasing number of series-connected converter cells. Finally, the scaling laws of the individual magnetic components are combined, which allows to make a final statement about how the total volume of the galvanically isolated ML converter changes with the number of cells. Even though the scaling laws are derived based on a simple galvanically isolated buck/boost converter topology, the general scaling trends found are not limited to this specific topology, but rather apply to any galvanically isolated ML converter structure.

## I. INTRODUCTION

The positive impact of multi-level (ML) converter topologies on the size of the filter components, especially the filter inductors, is well known for a long time and is also being used more and more often in power electronic products [1]–[4]. By means of several identical series-connected converter cells, it is possible to generate a switched voltage that has a certain DC or low-frequency (LF) voltage component and at the same time only a relatively small high-frequency (HF) rectangular voltage ripple. The small HF voltage ripple then appears across a common filter inductor, whereby the resulting voltage-time areas are significantly smaller than in conventional two-level converter topologies. This is exemplarily shown in **Fig. 1**

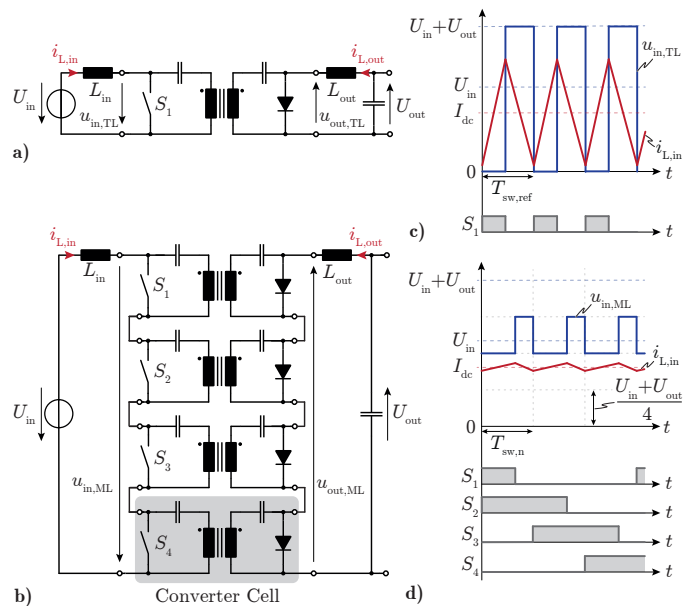


**Fig. 1.** a) Simple galvanically isolated buck/boost converter topology and b) the corresponding multi-level (ML) topology consisting of an input inductor  $L_{in}$ , multiple identical converter cells, each comprising a transformer, a switch, a diode and two blocking capacitors, and an output inductor  $L_{out}$ , with the characteristic waveforms of the input inductor  $L_{in}$  for both topologies shown in c) and d), respectively. The topology is exemplarily shown for four converter cells, but can consist of any number of cells.

by means of the voltage and current waveforms of the input inductor  $L_{in}$  of a galvanically isolated single-stage buck/boost converter topology [5]. Hence, in **Fig. 1a** the topology is shown as a simple two-level converter with

$$u_{in,TL} = x \cdot (U_{in} + U_{out}), \quad x \in \{0, 1\}, \quad (1)$$

whereby a conducting input side switch results in a voltage of  $+U_{in}$  across  $L_{in}$ , whereas a blocking input side switch results in a voltage of  $-U_{out}$  across  $L_{in}$ , if a 1:1 turns ratio of the transformer is assumed (cf. **Fig. 1c**). The same applies to the output inductor  $L_{out}$ , which is why identical flux linkages

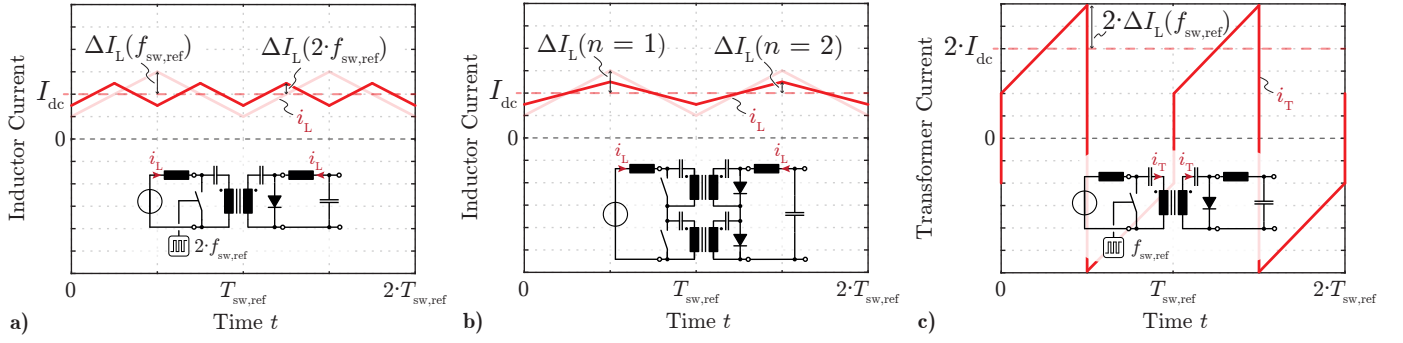


**Fig. 2.** **a)** Inductor current in the *reference system* with a switching frequency of  $f_{sw,ref}$  (transparent line) and  $2 \cdot f_{sw,ref}$  (solid line). **b)** Inductor current in the *reference system* (transparent line) and a dual-cell converter (solid line) with the same effective switching frequencies of  $f_{sw,ref}$ . **c)** Transformer current in the *reference system* with a switching frequency of  $f_{sw,ref}$  (solid line).

in the two inductors occur. Furthermore, the input side and output side series-capacitor voltages correspond to  $U_{in}$  and  $U_{out}$ , respectively, which is necessary to avoid saturation of the transformer core and results from the steady-state volt-second balance of the input and output inductors. This simple two-level converter is operated with a constant switching frequency  $f_{sw,ref}$  and is referred to as *reference system* in the remainder of the paper, since all scaling laws which will be derived are related to this converter.

The same topology is implemented in **Fig. 1b** as an ML converter, where e.g. four identical galvanically isolated converter cells ( $n = 4$ ) are connected in series, whereby three additional voltage levels are available at the output-side terminal of  $L_{in}$ , according to

$$u_{in,ML} = x \cdot \frac{U_{in} + U_{out}}{4}, \quad x \in \{0, \dots, 4\}. \quad (2)$$

Consequently, a much smaller voltage ripple  $\Delta u_{L,in} = U_{in} - u_{in,ML}$  is applied across  $L_{in}$  compared to the *reference system*, which is why the inductor volume can be significantly reduced, even for the same number of overall switching operations per second (identical frequencies of  $\Delta u_{L,in}$ ) as shown in **Fig. 1d**. As already mentioned, the advantageous scaling of the volumes of the filter components in non-isolated ML converters is well known and actively used, however, it has not yet been investigated in detail how the *total* volume of the magnetic components in galvanically isolated converter systems is affected by the ML approach, and whether the advantageous scaling also applies to the transformers that provide the required galvanic isolation. In this paper, in **Sec. II**, scaling laws for the inductor volume in ML converter systems are first derived before the same procedure is used in **Sec. III** to find scaling laws for the transformer volumes as well. Finally, in **Sec. IV**, the volumes of the two magnetic components are combined and the resulting scaling law of the total volume of the magnetic components in galvanically isolated ML converter systems is analyzed and discussed in detail. **Sec. V** concludes the findings of this paper.

## II. SCALING OF THE INDUCTOR VOLUME

The approximate volume of an inductor depends primarily on the (rms) current to be carried in the particular application ("electrical design") and the inductance value required to limit the current ripple due to the applied AC voltage, or equivalently, on the peak current relevant for the "magnetic" dimensioning of the component. This dependency can be derived from the so-called area product [6,7], which is usually used for a pre-selection of suitable inductor cores and consists of the product of the minimum cross-sectional area  $A_C$  of a specific inductor core geometry and the respective available winding window  $A_W$ , according to

$$A_C \cdot A_W = \frac{L \cdot I_{pk} \cdot I_{rms}}{k_W \cdot B_{sat} \cdot J_{rms}} \rightarrow V_L \propto (A_C \cdot A_W)^{\frac{3}{4}}, \quad (3)$$

where  $I_{pk}$ ,  $I_{rms}$ ,  $L$ ,  $k_W$ ,  $B_{sat}$  and  $J_{rms}$  denote the peak current, the maximum rms current, the inductance, the winding filling factor, the saturation flux density of the core material, and the maximum allowable current density in the winding, respectively. Hence, the area product depends on electrical properties ( $I_{pk}$  and  $I_{rms}$ ), the desired inductance value ( $L$ ), and geometrical and material properties ( $k_W$ ,  $B_{sat}$ , and  $J_{rms}$ ), where the latter do not directly depend on the number of converter cells  $n$  (for higher  $n$  the magnetic components are showing a higher surface to volume ratio and therefore would e.g. allow higher conduction losses and/or higher  $J_{rms}$  [7]), which is why they can be considered as constants. In order to be able to deduce the volume  $V_L$  of the inductor (in  $[m^3]$ ) from the area product (in  $[m^4]$ ), the area product must finally be raised to the power of  $3/4$ , according to (3).

As can be seen in **Figs. 2ab**, both  $I_{pk}$  and  $I_{rms}$  vary with the effective switching frequency  $f_{sw,n}$  and with the number of converter cells  $n$ , which is why these two parameters must be expressed in terms of  $f_{sw,n}$  and  $n$  in order to be able to estimate the influence of the ML approach on the inductor volume. Note, that the term "effective switching frequency" is used in the following for that frequency which is present across the inductor and thus determines the frequency of the current ripple. Hence, the effective switching frequency of an ML converter system corresponds to  $n$  times the switching frequency of a single converter cell, due to the assumed mutually

phase-shifted (interleaved) modulation of the converter cells. According to **Figs. 2ab**, the peak current  $I_{pk}$  corresponds to the sum of the average inductor current  $I_{dc}$  and the amplitude of the occurring (single-side) current ripple  $\Delta I_L$ , while the rms value of the triangular current can be calculated, according to

$$I_{pk} = I_{dc} + \Delta I_L \quad \text{and} \quad I_{rms} = \sqrt{I_{dc}^2 + \frac{\Delta I_L^2}{3}}. \quad (4)$$

Since the current ripple amplitude  $\Delta I_L$  depends on the design of the *reference system* ( $n = 1$ ), it is best to express this term as a fraction of the DC current, in order to keep a certain level of generality, according to

$$\Delta I_L = x \cdot I_{dc}. \quad (5)$$

However, if the effective switching frequency  $f_{sw,n}$  or the number of cells  $n$  in a converter system is increased or decreased, the current ripple amplitude  $\Delta I_L$  and, therefore, the current ripple factor  $x$  changes as well. As a first approximation, it can be assumed that  $x$  scales inversely proportional to  $n$  and  $f_{sw,n}$  since both an increase in  $n$  and  $f_{sw,n}$  result in a reduction of the voltage-time areas across the inductors (cf. **Figs. 2ab**). Consequently, the ratio between  $x(1, f_{sw,ref})$  of the *reference system* with a single converter cell and a switching frequency of  $f_{sw,ref}$  and  $x(n, f_{sw,n})$  of a converter with  $n$  converter cells, which is operated with an effective switching frequency of  $f_{sw,n}$ , can be expressed as

$$\frac{x(1, f_{sw,ref})}{x(n, f_{sw,n})} = \frac{n}{1} \cdot \frac{f_{sw,n}}{f_{sw,ref}}. \quad (6)$$

Due to the phase-shifted control (interleaving) of converter cells in ML converter systems, the actual current ripple in the inductors depends heavily on the ratio between the output and input voltage. This relationship is illustrated in **Fig. 3**, which shows the flux linkages applied to the inductors for different numbers of cells  $n$ , where an exemplary effective switching frequency of 1 Hz, an input voltage  $U_{in}$  of 1 V, and 1:1 transformers are assumed for simplicity reasons. However, since in most applications a certain input and/or output voltage range needs to be covered, the inductors need to be designed for the worst-case operating conditions within this range, thus, e.g. the maximum occurring peak current  $I_{pk}$ , which can be approximately estimated based on the current ripple factor scaling of (6).

Accordingly, using the aforementioned current ripple factor  $x$ ,  $I_{pk}$  and  $I_{rms}$  of (4) can be expressed as

$$I_{pk} = I_{dc} \cdot (1 + x) \quad \text{and} \quad I_{rms} = \sqrt{I_{dc}^2 \cdot \left(1 + \frac{x^2}{3}\right)}, \quad (7)$$

resulting in the area product ratio of the inductor in an ML converter with  $n$  converter cells and an effective switching

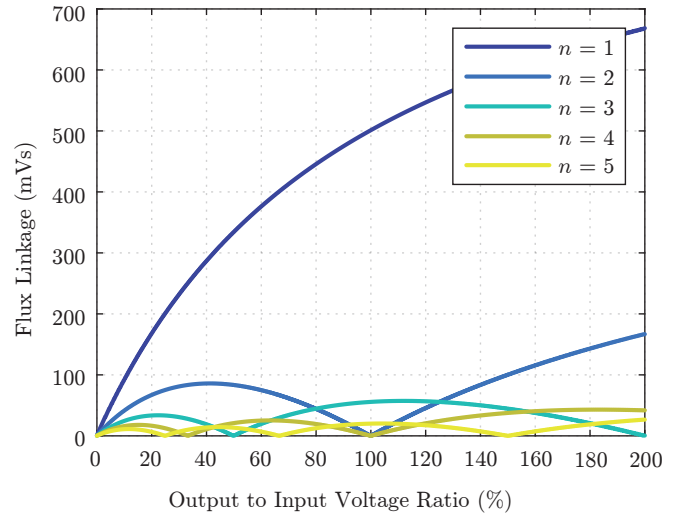


**Fig. 3.** Flux linkages applied to the inductors of the buck/boost converter topology shown in **Fig. 1** for different numbers of cells  $n$ , a constant exemplary input voltage  $U_{in}$  of 1 V, an effective switching frequency of 1 Hz, and different output to input voltage ratios.

frequency of  $f_{sw,n}$  and the inductor of the *reference system*, according to

$$\begin{aligned} \frac{(A_C \cdot A_W)(n, f_{sw,n})}{(A_C \cdot A_W)(1, f_{sw,ref})} &= \frac{(I_{pk} \cdot I_{rms})(n, f_{sw,n})}{(I_{pk} \cdot I_{rms})(1, f_{sw,ref})} \\ &= \frac{1 + \frac{x_{ref}}{n \cdot f}}{1 + x_{ref}} \cdot \sqrt{\frac{3 + \frac{x_{ref}^2}{n^2 \cdot f^2}}{3 + x_{ref}^2}}, \end{aligned} \quad (8)$$

where  $f$  denotes the ratio of the two effective switching frequencies, according to

$$f = \frac{f_{sw,n}}{f_{sw,ref}}, \quad (9)$$

and  $x_{ref}$  denotes the current ripple factor of the *reference system*, according to

$$x_{ref} = x(1, f_{sw,ref}). \quad (10)$$

Based on the area product ratio, the inductor volume ratio can then be determined, according to

$$\frac{V_L(n, f_{sw,n})}{V_L(1, f_{sw,ref})} = \left( \frac{1 + \frac{x_{ref}}{n \cdot f}}{1 + x_{ref}} \cdot \sqrt{\frac{3 + \frac{x_{ref}^2}{n^2 \cdot f^2}}{3 + x_{ref}^2}} \right)^{\frac{3}{4}}, \quad (11)$$

which is shown graphically in **Fig. 4**. The beneficial scaling of the inductor volume with increasing number of cells  $n$  and the effective switching frequency  $f_{sw,n}$  is evident, but can be shown even more clearly by calculating the minimum effective switching frequency for a certain given  $n$ , which results in identical inductor volumes of the *reference system* and the ML converter, according to

$$\frac{V_L(n, f_{sw,n})}{V_L(1, f_{sw,ref})} = 1, \quad (12)$$

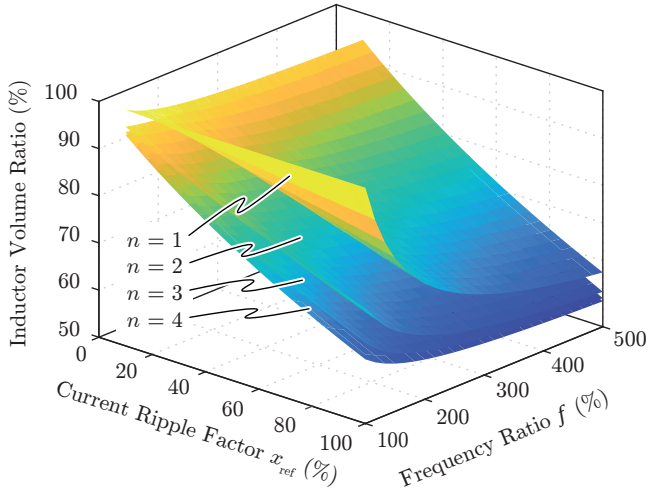


**Fig. 4.** Ratio between the volume of the inductors in the *reference system* with a switching frequency  $f_{sw,ref}$  and the inductors of an ML converter with  $n$  converter cells and an effective switching frequency  $f_{sw,n}$  for different inductor current ripple factors  $x_{ref}$  of the *reference system*, whereby the frequency ratio is given as  $f = \frac{f_{sw,n}}{f_{sw,ref}}$ .

which is achieved if

$$n \cdot f = 1, \quad (13)$$

and, therefore

$$n \cdot f_{sw,n} = f_{sw,ref}, \quad (14)$$

holds (cf. (11)). The results are shown in **Fig. 5**, where it can be seen, for example, that in a five-cell converter a frequency ratio  $f$  of only 20 % is required to obtain the same inductor volume as in the *reference system* ( $n = 1$ ) with five times the switching frequency (cf. gray markers in **Fig. 5**). Thus, the

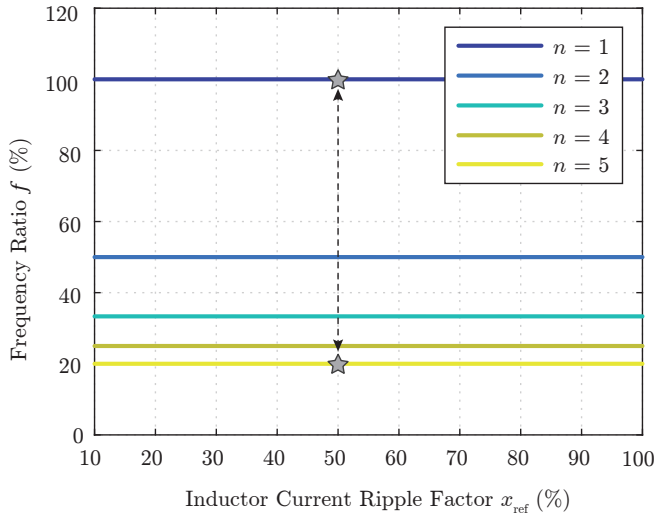


**Fig. 5.** Ratio between the effective switching frequency  $f_{sw,n}$  of a ML converter with  $n$  converter cells and the switching frequency  $f_{sw,ref}$  of the *reference system*, where the volumes of the inductors of both systems are identical, i.e.  $V_L(1, f_{sw,ref}) = V_L(n, f_{sw,n})$ .

inductors clearly benefit from the multi-level approach, which is why this approach is often used in practical applications. However, since many applications also require galvanic isolation, usually achieved by means of transformers, the following section examines whether these components also benefit from the ML approach in a similar way.

### III. SCALING OF THE TRANSFORMER VOLUME

Similar to the previously discussed inductors, the transformer volume can be estimated using the potentiated area product, with the electrical properties now being twice the rms current  $I_{rms}$  (due to the two windings) and the maximum flux linkage  $\Psi_{pk} = L_m \cdot I_{m,pk}$  (with  $L_m$  and  $I_{m,pk}$  being the the magnetizing inductance and the maximum magnetizing current), according to

$$A_C \cdot A_W = \frac{2 \cdot \Psi_{pk} \cdot I_{rms}}{k_W \cdot B_{sat} \cdot J_{rms}} \rightarrow V_T \propto (A_C \cdot A_W)^{\frac{3}{4}}, \quad (15)$$

where  $k_W$ ,  $B_{sat}$ , and  $J_{rms}$  denote the geometrical/material properties of the core: winding filling factor, saturation flux density, and maximum allowable current density, respectively [6]. The electrical properties can be calculated according to

$$\Psi_{pk} = \frac{D \cdot U_{in}}{f_{sw}} \quad \text{and} \quad I_{rms} = \sqrt{4 \cdot I_{dc}^2 + \frac{4 \cdot \Delta I_L^2}{3}}, \quad (16)$$

(cf. **Fig. 2c**) where  $D$  denotes the duty cycle of the converter cells. Taking into account the inductor current ripple factor  $x$ ,  $I_{rms}$  can be simplified to

$$I_{rms} = \sqrt{4 \cdot I_{dc}^2 \cdot \left(1 + \frac{x^2}{3}\right)}. \quad (17)$$

Considering the flux linkage and the rms current of a single transformer in an ML converter, which are given by

$$\Psi_{pk} = \frac{D \cdot U_{in}}{n \cdot \frac{f_{sw,eff}}{n}} \quad \text{and} \quad I_{rms} = \sqrt{4 \cdot I_{dc}^2 \cdot \left(1 + \frac{x_{ref}^2}{3 \cdot n^2 \cdot f^2}\right)}, \quad (18)$$

the area product ratio of a single transformer of an ML converter with  $n$  converter cells and an effective switching frequency of  $f_{sw,n}$  and the transformer of the *reference system* ( $n = 1$ ), can be calculated according to

$$\begin{aligned} \frac{(A_C \cdot A_W)(n, f_{sw,n})}{(A_C \cdot A_W)(1, f_{sw,ref})} &= \frac{(\Psi_{pk} \cdot I_{rms})(n, f_{sw,n})}{(\Psi_{pk} \cdot I_{rms})(1, f_{sw,ref})} \\ &= \frac{1}{f} \cdot \sqrt{\frac{3 + \frac{x_{ref}^2}{n^2 \cdot f^2}}{3 + x_{ref}^2}}. \end{aligned} \quad (19)$$

where  $f$  and  $x_{ref}$  again denote the ratio of the two effective switching frequencies according to (9), and the inductor current ripple factor of the *reference system*.

Based on the area product ratio, the total transformer volume ratio can be determined, according to

$$\frac{V_T(n, f_{sw,n})}{V_T(1, f_{sw,ref})} = n \cdot \left( \frac{1}{f} \cdot \sqrt{\frac{3 + \frac{x_{ref}^2}{n^2 \cdot f^2}}{3 + x_{ref}^2}} \right)^{\frac{3}{4}} \quad (20)$$

which is shown graphically in **Fig. 6**. The factor  $n$  in (20) is due to the fact that a separate transformer is required for each converter cell, which is why,  $n$  times the volume of a transformer must be taken into account when comparing the total transformer volumes.

It is evident that an increase in  $f$  reduces the total volume of the transformers, but in contrast to the inductors, an increase in the number of cells  $n$  greatly increases the total transformer volume. The disadvantageous scaling becomes even more obvious if, as in **Fig. 5** for the inductors, the minimum required switching frequency is calculated, which would be necessary such that the total transformer volume of an ML converter with  $n$  converter cells does not exceed the volume of the transformer of the *reference system* (cf. **Fig. 7**). Thus, for e.g. a five-cell converter with an inductor current ripple factor  $x_{\text{ref}}$  of the *reference system* of 50%, at least an eight times higher effective switching frequency is required compared to the *reference system*, if the total volume of the five transformers should not be larger than the single transformer of the *reference system* (cf. gray markers in **Fig. 7**).

Consequently, it is clear that on the one hand, the ML approach is beneficial for the inductor volume, but on the other hand, the transformer volume increases significantly with  $n$ . Therefore, considering the example at hand (cf. **Fig. 1**), it depends on the distribution of the total volume  $V_{\text{ref}}$  of the magnetic components in the *reference system* between the two inductors ( $V_{L,\text{ref}}$ ) and the transformer ( $V_{T,\text{ref}}$ ), whether the ML approach leads to a reduction or an increase in the total volume for a given effective switching frequency, as will be shown in

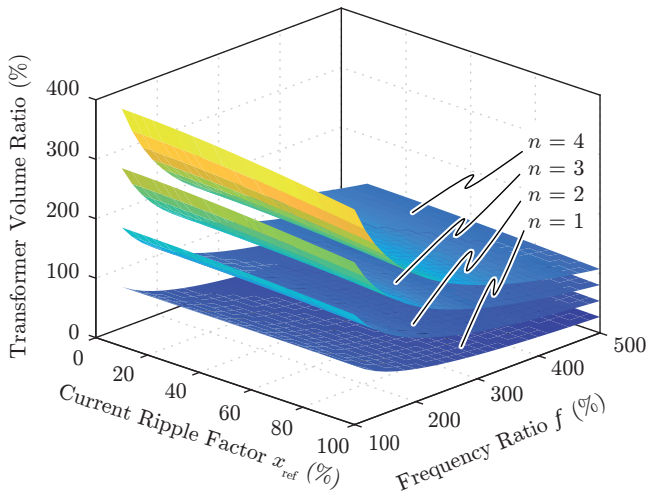


**Fig. 6.** Ratio between the volume of the transformer in the *reference system* ( $n = 1$ ) with an switching frequency  $f_{\text{sw,ref}}$  and the total volume of the transformers in an ML converter with  $n$  converter cells and an effective switching frequency  $f_{\text{sw},n}$  for different inductor current ripple factors  $x_{\text{ref}}$  of the *reference system*, whereby the frequency ratio is given as  $f = \frac{f_{\text{sw},n}}{f_{\text{sw,ref}}}$ .

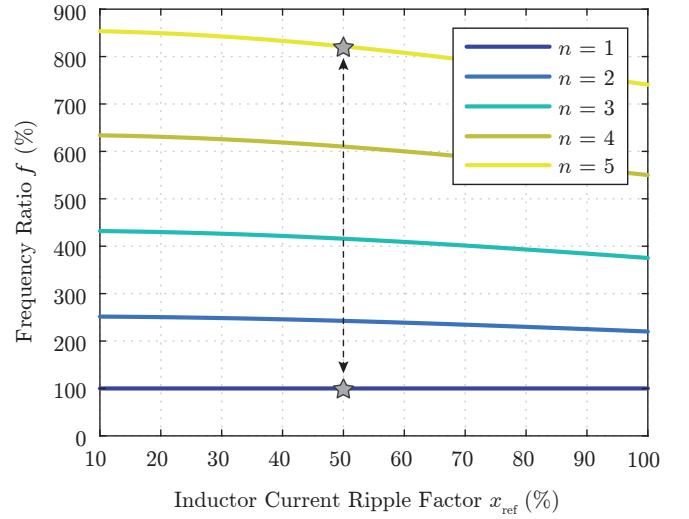


**Fig. 7.** Ratio between the effective switching frequency  $f_{\text{sw},n}$  of a ML converter with  $n$  converter cells and the switching frequency  $f_{\text{sw,ref}}$  of the *reference system*, where the total transformer volumes of both systems are identical, i.e.  $V_{\text{T}}(1, f_{\text{sw,ref}}) = V_{\text{T}}(n, f_{\text{sw},n})$ .

the following.

#### IV. SCALING OF THE TOTAL MAGNETICS VOLUME

Assuming an initial volume distribution of

$$V_{L,\text{ref}} = \gamma \cdot V_{\text{ref}} \quad \text{and} \quad V_{T,\text{ref}} = (1 - \gamma) \cdot V_{\text{ref}}, \quad (21)$$

with  $\gamma \in (0, 1)$ ,  $V_{L,\text{ref}}$  being the total volume of the two inductors of the *reference system* and  $V_{T,\text{ref}}$  being the volume of the transformer of the *reference system*, the scaling of the total magnetics volumes can be expressed as

$$\begin{aligned} \frac{V_n(n, f_{\text{sw},n})}{V_{\text{ref}}(1, f_{\text{sw,ref}})} &= \underbrace{\gamma \cdot \left( \frac{1 + \frac{x_{\text{ref}}}{n \cdot f}}{1 + x_{\text{ref}}} \cdot \sqrt{\frac{3 + \frac{x_{\text{ref}}^2}{n^2 \cdot f^2}}{3 + x_{\text{ref}}^2}} \right)^{\frac{3}{4}}}_{\text{Inductor Volume}} \\ &+ \underbrace{(1 - \gamma) \cdot n \cdot \left( \frac{1}{f} \cdot \sqrt{\frac{3 + \frac{x_{\text{ref}}^2}{n^2 \cdot f^2}}{3 + x_{\text{ref}}^2}} \right)^{\frac{3}{4}}}_{\text{Transformer Volume}}, \quad (22) \end{aligned}$$

(where  $V_n(n, f_{\text{sw},n})$  denotes the total volume of the magnetic components of the ML converter) which is shown in **Fig. 8** for three different exemplary volume distributions  $\gamma$  of the *reference system*. From this graph it can be seen that even if 75% of the total magnetics volume in the *reference system* is occupied by the inductors, the total magnetics volume increases significantly as the number of cells increases for a given effective switching frequency. Alternatively, the effective switching frequency needs to be increased for higher numbers of cells in order to keep the total magnetics volume of the ML converter the same as in the *reference system*.

However, the volume distribution of the *reference system*

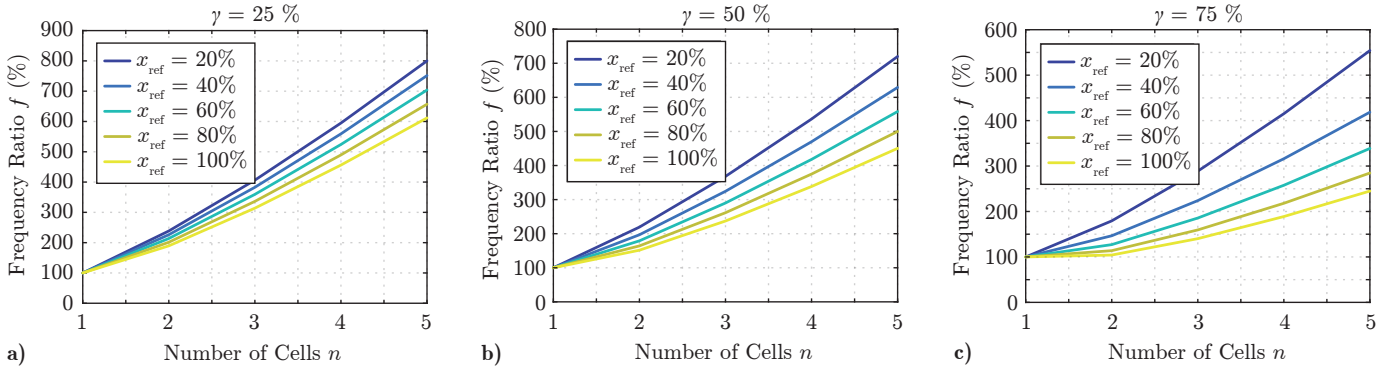


**Fig. 8.** Minimum required effective switching frequency ratio  $f$  to keep a certain total magnetics volume (sum of inductor and transformer volumes, cf. Fig. 1) with increasing the number of cells  $n$  for exemplary volume distributions of the *reference system* of **a)**  $\gamma = 25\%$ , **b)**  $\gamma = 50\%$ , and **c)**  $\gamma = 75\%$ , according to (21).

cannot be arbitrarily chosen, as it is directly given by the area products of (3) and (15) if identical core materials, cooling conditions, etc. for the inductors and the transformers are assumed, as will be shown in the following.

If the inductance in (3) is replaced by

$$L = \frac{U_{in}}{4 \cdot f_{sw,ref} \cdot x_{ref} \cdot I_{dc}}, \quad (23)$$

where, without loss of generality, a duty cycle of 50% is assumed, the following volume ratio  $\chi$  between the two inductors and the transformer of the *reference system* can be found

$$\frac{V_{L,ref}}{V_{T,ref}} = \frac{2 \cdot (A_C \cdot A_w)_L^{\frac{3}{4}}}{(A_C \cdot A_w)_T^{\frac{3}{4}}} = \frac{(1 + x_{ref})^{\frac{3}{4}}}{2^{\frac{5}{4}} \cdot x_{ref}^{\frac{3}{4}}} = \chi, \quad (24)$$

as shown in **Fig. 9**. The inductor volume share  $\gamma$  of the

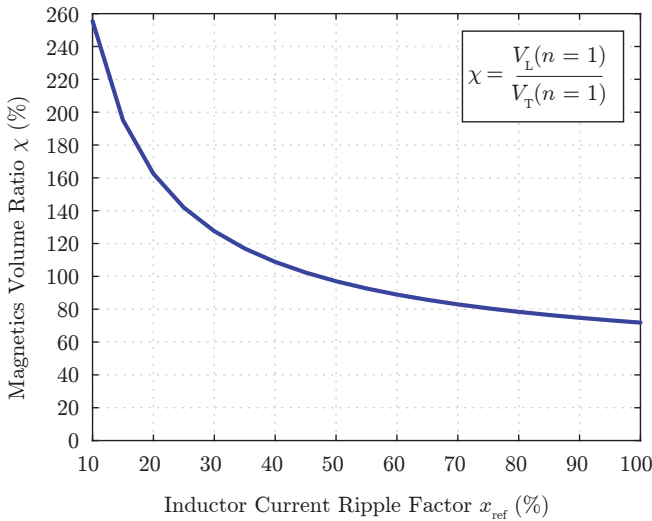


**Fig. 9.** Volume distribution  $\chi$  between the inductors and the transformer in the *reference system* ( $n = 1$ ) for different inductor current ripple ratios  $x_{ref}$ .

*reference system* can now be calculated based on  $\chi$  and (21) to

$$\gamma = \frac{\chi}{1 + \chi}, \quad (25)$$

which in combination with (22) results in the final scaling law for isolated single-stage multi-level buck/boost converter topologies:

$$\frac{V_n(n, f_{sw,n})}{V_{ref}(1, f_{sw,ref})} = \left( \frac{3 \cdot n^2 \cdot f^2 + x_{ref}^2}{3 + x_{ref}^2} \right)^{\frac{3}{2}} \cdot \frac{1}{(n \cdot f)^{\frac{3}{2}}} \cdot \frac{4 \cdot x_{ref}^{\frac{3}{4}} \cdot n^{\frac{7}{4}} + 2^{\frac{3}{4}} \cdot (n \cdot f + x_{ref})^{\frac{3}{4}}}{4 \cdot x_{ref}^{\frac{3}{4}} + 2^{\frac{3}{4}} \cdot (1 + x_{ref})^{\frac{3}{4}}}. \quad (26)$$

In **Fig. 10**, the minimum effective switching frequency is shown for different numbers of cells  $n$  and different inductor current ripple factors  $x_{ref}$  of the *reference system*, which is required to keep the total magnetics volume the same according to (26). Alternatively, the total magnetics volume ratio can be calculated for different numbers of cells  $n$  and different inductor current ripple factors  $x_{ref}$  of the *reference system* for identical effective switching frequencies  $f_{sw,n}$ , as shown in **Fig. 11**.

It can be concluded that no advantages can be achieved with regard to the magnetic components in galvanically isolated systems when the ML approach is used. Consequently, from a magnetic component perspective, it is more reasonable to build a galvanically isolated DC/DC converter as a two-stage system consisting, for example, of a non-isolated multi-level buck/boost converter whose input and output inductors become significantly smaller thanks to the ML approach, which is followed by a two-level DC-transformer (DCX), which ensures the required galvanic isolation. Such a DCX is usually implemented as a series-resonant converter which is always operated at (or slightly above) its resonant frequency, allowing it to be built extremely efficiently and with high power density [8].

In order to visualize the disadvantageous scaling of the total volume of the magnetic components in isolated ML converter systems, the magnetic components of a unity gain *reference*

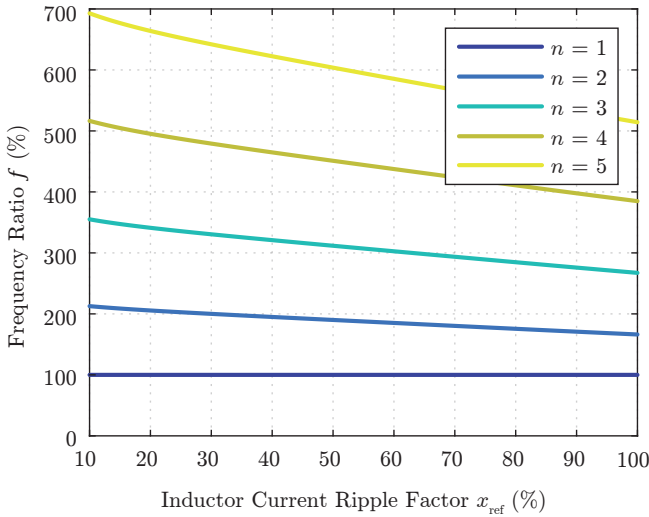


**Fig. 10.** Ratio between the effective switching frequency  $f_{sw,n}$  of a ML converter with  $n$  converter cells and the switching frequency  $f_{sw,ref}$  of the *reference system*, where the total magnetics (inductors and transformers) volumes of both systems are identical.

*system* were built for an exemplary nominal output power  $P_n$  of 3.3kW, an input voltage  $U_{in} (= U_{out})$  of 400 V, an effective switching frequency of 100kHz and an inductor current ripple factor  $x_{ref}$  of 50%, as shown in **Fig. 12a**. For comparison, an ML converter with  $n = 4$  cells was designed for the same specifications and the same number of total switching operations per second ( $f_{sw,n} = f_{sw,ref}$ ), and the respective magnetic components were built (cf. **Fig. 12b**). To keep the comparison fair, only solid wire windings and conventional E-cores made of ferrite were considered for the

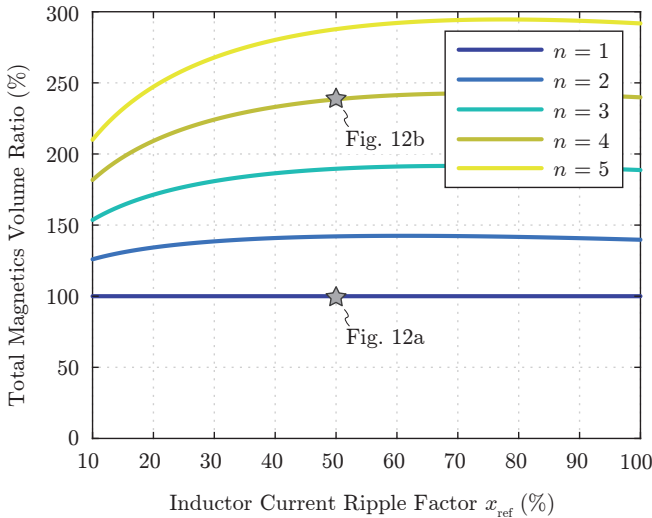


**Fig. 11.** Ratio between the total magnetics volume of a ML converter with  $n$  converter cells and the total magnetics volume of the *reference system* ( $n = 1$ ) for the same effective switching frequency  $f_{sw,n}$ . The stars indicate the volume ratio of the design examples of **Fig. 12a** and **Fig. 12b**.

design of the magnetic components. The specifications  $P_n$  and  $U_{in}$  were chosen in such a way that the area products of the E-cores used are at most 10% larger than what is required according to (3) and (15). In **Fig. 12**, it can be seen that although the volumes of the individual components are slightly smaller in the ML converter, the increased number of transformers results in a significant increase in the total volume of the magnetics if the ML approach is used (cf. **Table I**). Furthermore, the increased material volume of copper and ferrite in the ML converter, which are exposed to approximately the same currents and flux densities as in the *reference system* (cf. (16) and (18)), leads to a significant increase in losses in the ML converter.

The fact that the ML approach is not immediately sensible in galvanically isolated converter systems can also be easily understood conceptually, since the idea behind the ML approach of generating a voltage with the highest possible ratio between DC (or LF) component and high-frequency ripple is diametrically opposed to what is required to transfer power through a transformer, since the excitation voltage applied to a transformer needs to be mean-free. This is also the reason why each converter cell requires its own transformer, since in a single-stage ML (DC/DC) converter only the respective cell-internal voltages are mean-free. However, due to the reduced cell-internal switching frequency of  $f_{sw,n}/n$  and the reduced cell-internal port voltages of  $U_{in}/n$ , each transformer of the ML converter needs to be designed for the same flux linkage

$$\Psi_{pk} = \frac{U_{in}}{n} \cdot \frac{n}{f_{sw,n}} = \frac{U_{in}}{f_{sw,n}} \quad (27)$$

and almost the same rms current  $I_{rms}$  as the transformer of

Inductors		
	Reference System	Multi-Level System
Inductance	200 $\mu$ H	200 $\mu$ H
Core	E36/18/11 (N87)	E34/14/9 (N87)
Number of Turns	54	57
Wire Diameter	1.7 mm	1.6 mm
Box Volume per Inductor	31.7 cm <sup>3</sup>	25.4 cm <sup>3</sup>
Losses per Inductor	11.6 W	9.2 W
Transformers		
	Reference System	Multi-Level System
Core	E47/20/16 (N87)	E42/21/15 (N87)
Number of Turns	$N_{pri} = N_{sec} = 19$	$N_{pri} = N_{sec} = 25$
Wire Diameter	2.2 mm	2.1 mm
Box Volume per Transf.	59.6 cm <sup>3</sup>	52.5 cm <sup>3</sup>
Losses per Transformer	24.8 W	22.7 W
Magnetics of the Total System		
	Reference System	Multi-Level System
Components	2 Induc., 1 Transf.	2 Induc., 4 Transf.
Total Box Volume	123 cm <sup>3</sup>	261 cm <sup>3</sup>
Total Losses	48 W	109 W

**Table I**

Specifications of the magnetic components of **Fig. 12** with the respective occurring losses under nominal operating conditions ( $U_{in} = U_{out} = 400$  V,  $P_n = 3.3$  kW,  $f_{sw,ref} = f_{sw,n} = 100$  kHz, and  $x_{ref} = 50$  %).

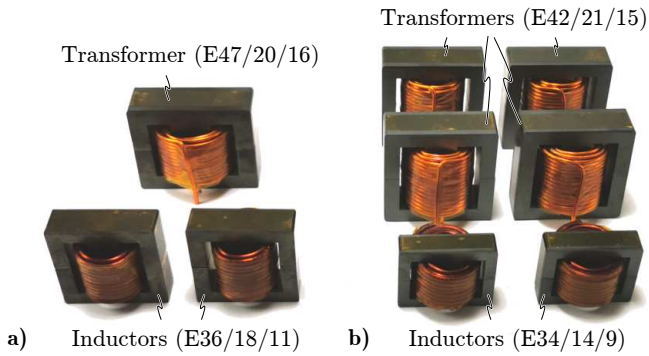


**Fig. 12.** Magnetic components of **a)** a reference system ( $n = 1$ ) with a nominal power of 3.3 kW, a nominal input voltage of 400 V, an effective switching frequency of 100 kHz and a current ripple factor  $x_{ref}$  of 50%, and **b)** an equivalent multi-level converter with four converter cells ( $n = 4$ ) for the same specifications.

the reference system, since only the current ripple ( $2 \cdot \Delta I_L$ ) is affected by the ML approach, but not the average value of the trapezoidal transformer current  $i_T$  of  $2 \cdot I_{dc}$  (cf. Fig. 2c). The transformer of an ML cell is therefore only marginally smaller than the transformer of the reference system, which inevitably leads to a significant increase in the total volume of the transformers in ML converter systems (cf. Fig. 12). Consequently, the validity of the above general findings is not limited to the buck/boost converter topology of Fig. 1a, and the findings must be considered as a general trend for all galvanically isolated ML converter topologies.

## V. CONCLUSION

The derived scaling laws for the volumes of the magnetic components in isolated multi-level (ML) converter systems clearly reveal, that using multiple voltage levels yields significant advantages regarding inductor volume, but at the same time increases the total transformer volume substantially. Furthermore, the disadvantageous scaling of the transformer volume with increasing numbers of cells  $n$  outweighs the benefits in terms of inductor volume, which is why the overall volume of the magnetic components increases with increasing  $n$ . Consequently, it can be stated that from a magnetic component perspective the ML approach in general is not suitable for galvanically isolated single-stage converter systems. Even though the scaling laws were derived based on the simple and universal area products and specific to a galvanically isolated buck/boost converter topology, the general scaling trends apply to any galvanically isolated ML converter topology, since the ML approach has a positive effect on the volume of filter components, but always has exactly the opposite effect on the transformer volume, independent of the actual converter topology.

The ML approach therefore only makes sense if, for example, the input voltage is too high to be handled with a single ( $n = 1$ ) converter cell, as is the case with e.g. solid-state transformers [9] (where the modularization penalty is also a known issue [10]). Another reason for the application of the ML approach

could be the economy of scale or the manufacturing of smaller, more easily transportable and manageable units which can be used for the assembly of a high-power system, where the adverse scaling of the magnetic components could be tolerated.

## REFERENCES

- [1] T. Modeer, C. B. Barth, N. Pallo, W. H. Chung, T. Foulkes, and R. C. N. Pilawa-Podgurski, "Design of a gan-based, 9-level flying capacitor multilevel inverter with low inductance layout," in *IEEE Applied Power Electronics Conference and Exposition (APEC)*, 2017, pp. 2582–2589.
- [2] A. D. B. Lange, T. B. Soeiro, M. S. Ortmann, and M. L. Heldwein, "Three-level single-phase bridgeless pfc rectifiers," *IEEE Transactions on Power Electronics*, vol. 30, no. 6, pp. 2935–2949, 2015.
- [3] S. Qin, Y. Lei, Z. Ye, D. Chou, and R. C. N. Pilawa-Podgurski, "A high-power-density power factor correction front end based on seven-level flying capacitor multilevel converter," *IEEE Journal of Emerging and Selected Topics in Power Electronics*, vol. 7, no. 3, pp. 1883–1898, 2019.
- [4] M. Kasper, D. Bortis, and J. W. Kolar, "Scaling and balancing of multi-cell converters," in *International Power Electronics Conference (IPEC-Hiroshima 2014 - ECCE ASIA)*, 2014, pp. 2079–2086.
- [5] R. D. Middlebrook and S. Cuk, "Isolation and multiple output extensions of a new optimum topology switching dc-to-dc converter," *IEEE Power Electronics Specialists Conference*, pp. 256–264, 1978.
- [6] N. Mohan, T. M. Undeland, and W. P. Robbins, *Power Electronics: Converters, Applications, and Design*, 3rd ed. Wiley, 2002, ch. 30, Design of Magnetic Components, pp. 760–790.
- [7] C. R. Sullivan, B. A. Reese, A. L. F. Stein, and P. A. Kyaw, "On size and magnetics: Why small efficient power inductors are rare," in *International Symposium on 3D Power Electronics Integration and Manufacturing (3D-PEIM)*, 2016, pp. 1–23.
- [8] G. Deng, Y. Sun, G. Xu, X. Chen, S. Xie, S. Yan, M. Su, and Y. Liao, "Zvs analysis of half bridge llc-dcx converter considering the influence of resonant parameters and loads," in *IEEE Energy Conversion Congress and Exposition (ECCE)*, 2020, pp. 1186–1190.
- [9] J. W. Kolar and J. Huber, "Solid-state transformers - the slope of enlightenment," *Keynote in IEEE Southern Power Electronics Conference (SPEC)*, p. 32, 2022.
- [10] J. Huber, P. Wallmeier, R. Pieper, F. Schafmeister, and J. W. Kolar, "Comparative evaluation of mvac-lvdc sst and hybrid transformer concepts for future datacenters," in *International Power Electronics Conference (IPEC-Himeji - ECCE Asia)*, 2022, pp. 2027–2034.